JOURNAL OF MATERIALS SCIENCE 9 (1974) 934-940

Strength and fracture mechanisms in beta-alumina

R. STEVENS
Materials Science Section, The Electricity Council Research Centre, Capenhurst, Chester, UK

The fracture stress, fracture initiation energy and work of fracture have been measured for a fine grained beta-alumina ceramic. The fracture stress has been shown to be naturally distributed and can be described by the Weibull distribution function. Values of the fracture initiation energy and work of fracture were found to be similar, 25 J m^{-2}.

The microstructure of beta-alumina has been examined using transmission electron microscopy. In thin foils of the fine grained material cleavage cracks were invariably found to occur in the basal layers. The phenomena has been explained empirically in terms of atomic bonding of the mirror plane. Contributing terms to the fracture energy γ_T have been discussed and it is suggested that lamination and deformation at the crack tip by generation and movement of dislocations along basal planes is a significant factor.

1. Structure and composition of beta-alumina

The term β-Al_2O_3 is commonly used to describe a range of compositions in the Na_2O-Al_2O_3 system. The empirical formula $Na_2O.11\ Al_2O_3$ is given to one compound in the system [1]. The composition of the compound can be made to vary considerably and excessive amounts of sodium oxide may be present, resulting in a defect structure inconsistent with the empirical composition.

Further additions of sodium oxide yield another compound with the formula $Na_2O.5\ Al_2O_3$, β''-alumina [2]. Recently the compound with an approximate composition $Na_2.O,\ 8\ Al_2O_3$ has been described which has the same structure as β-alumina [3]; this structure has yet to be confirmed.

The crystal structure of β-Al_2O_3 ($Na_2O,\ 11\ Al_2O_3$) is hexagonal ($P6_3/mmc$) with $a_0 = 5.593$ and $c_0 = 22.610$. β''-alumina ($Na_2O,\ 5\ Al_2O_3$) has a similar structure with $a_0 = 5.601$ and $c_0 = 33.95$. The atomic arrangement consists of four layers of close packed oxygen ions, the aluminium ions occupying the positions usually taken up by the magnesium and aluminium ion in the spinel structure. The unit is, therefore, called a "spinel block" and has its $\langle 111 \rangle$ parallel to the c-axis of the β-Al_2O_3 unit cell, and has a repeat distance of ~11.23 Å.

The sodium ions lie in the plane parallel to the close packed oxygen ion plane, i.e. the basal plane of the β-Al_2O_3 unit cell. The oxygen and aluminium ion arrangement above and below this plane are mirror images, and the sodium containing plane is thus referred to as a "mirror plane". It is of interest to note the relatively large spacing of the oxygen-aluminium bonds in the mirror plane and the large separation of the spinel blocks (4.76 Å) across the mirror plane. The sodium ions reside in the mirror plane and, due to the large "holes" in the lattice, are able to move with relative ease. The high ionic mobility of the sodium ions has been a major factor in the recent interest in β-Al_2O_3.

The β'' structure is similar except that the unit cell is made of three spinel blocks, thus increasing the c_0 parameter. There are further small differences, which have been discussed adequately elsewhere [4].

2. Experimental techniques

Bars of β-alumina 10 cm × 1 cm × 0.5 cm were manufactured from powder stocks by isostatically pressing and sintering. The details of the process have been published previously [5]. Final density of the sintered bars was in the range 3210 to 3220 kg m^{-3}, effectively ~98% dense.

The bars were diamond ground and cut to the

required size and shape. Mechanical testing was carried out on an Instron tensile testing machine. Work of fracture measurements and crack initiation energies were measured and the methods used will be described later.

The fracture surfaces were examined using scanning and transmission electron microscopy both directly and by means of plastic carbon replicas. Thin foils of material for use in transmission electron microscopy were prepared. The technique involves diamond cutting and grinding of the β-Al_2O_3 to a thin wafer. The wafer $\simeq 0.02$ mm thick was then mounted on a glass slide using a thermosetting "Lakeside" resin cement and polished on a series of diamond pastes, finishing on 1 μm grade. Discs of the ceramic wafer were cut out using an ultrasonic drill and cleaned in methanol. The discs were then attached to single hole copper grids, again using Lakeside cement, and finally thinned on an Edwards ion-beam thinning unit.

3. Microstructure

The fine grain size of the material used in this study precluded the use of optical microscopy. Transmission electron microscopy showed the material to have grains in the size range 0.5 to 2 μm. A typical microstructure is seen in Fig. 1. There is uniformity of grain size over large areas, certain of the grains appearing longer due to morphological characteristics, the aspect ratio reaching a maximum where the *c*-direction lies in the foil plane. The grains are usually angular in shape, although occasionally one of round section may be seen. Invariably with this shape of grain it was found that the basal plane is parallel to the plane of the foil.

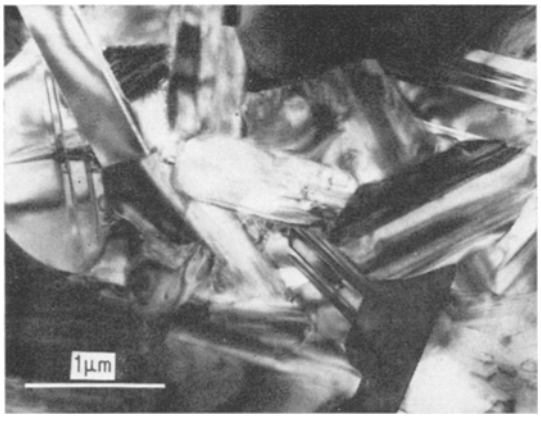

Figure 1 Typical microstructure of β-alumina used in the fracture tests.

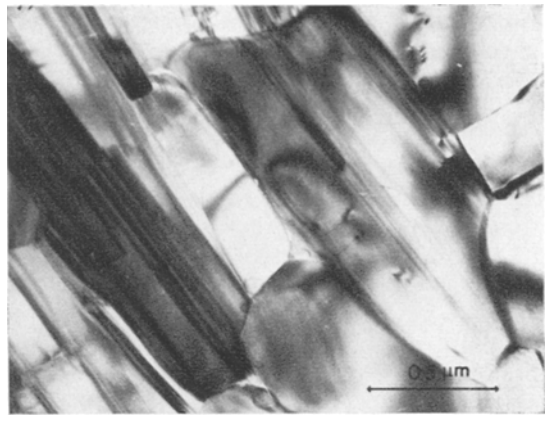

Figure 2 Planar defects associated with dislocations. The defects lie in the basal plane of β-alumina.

Little substructure in the form of sub-grain boundaries or dislocation tangles is present. The only defects present appear as bands parallel to $\langle\bar{2}110\rangle$ [6, 7]. These are believed to be the slip traces of dislocations lying in the basal plane [7], and can readily be seen in Fig. 2. In certain grains isolated dislocations without these slip traces are also present, but to a lesser extent.

4. Crack initiation and propagation

Griffith [8] formulated the equation relating the mechanical properties of a material to a defect present in the material. He related the tensile stress σ on an elliptical flow of length C in a material of elastic modulus E, and surface energy γ. Orowan [9] modified the equation to include a term allowing for plastic flow to occur at the crack tip, increasing the surface energy term to γ_T:

$$\sigma \simeq \sqrt{\left(\frac{2E\gamma_T}{C}\right)}.$$

The fracture initiation energy γ_i can be measured by the technique of Gilman [10]. The total energy expended in the fracture process can be measured by the work of fracture test [11]. Results for both types of test at room temperature are given below, the values quoted being the mean of several tests.

Fracture initiation energy $\gamma_i = 25$ J m^{-2} (s.d. = 7.1)

Work of fracture $\gamma_F = 26$ J m^{-2} (s.d. = 5.1)

Analysis of fracture energies in this manner are based on the assumptions that the material responds to an applied stress with a linear elastic expansion, and that the material is elastically isotropic. Very few materials exhibit such ideal behaviour. Because of its crystal structure one would expect β-alumina to be strongly anisotropic. However, the extremely fine grain size of the experimental material allows the assumption to be made, since fracture phenomena will be shown to be an order of magnitude larger (i.e. critical crack length $\sim 10 \times$ grain size) and due to natural distribution in grain orientation, the material can be considered to be elastically isotropic.

A number of processes take place at the crack tip during fracture initiation. They can be divided into two basic phenomena. Deformation can occur even in brittle materials due to the stress concentrations at crack tips causing dislocation generation and movement [12] and in certain cases mechanical twinning [13]. A topographical effect also occurs whereby the free surface energy is effectively increased by a factor ϵ due to subsidiary cracking and cleavage step formation. Thus

$$\gamma_I = \epsilon\gamma_s + \gamma_p$$

where γ_I is the crack initiation energy, γ_s the surface energy, ϵ a geometrical factor and γ_p the energy absorbed by plastic deformation.

5. Fracture strength

The fracture strength of brittle materials can be measured in numerous ways [14], the most common being three or four point bend tests and the ring test. Rings were cut from a 1.6 cm diameter tube of 1.5 mm wall thickness and fractured in compression in an Instron tensile testing machine. The fracture stress was then calculated according to thin walled elasticity theory [15]. Corrections were made for non-uniformity of wall thickness and eccentricity of the test rings where this was deemed necessary [16].

Analysis of strength data for brittle materials can be based on the maximum sized flaw concept, i.e. the weakest link will cause failure. On this basis Weibull [17] derived a probability function to describe this type of behaviour. The probability of failure at any stress, σ, is given by

$$F(\sigma) = 1 - e^{-B}$$

where

$$B = \iiint_v \left(\frac{\sigma - \sigma_u}{\sigma_0}\right)^m dV$$

and σ_u is considered as the zero stress, below which flaws do not propagate, σ_0 is the Weibull stress and m the Weibull modulus. The function relates to the whole of the volume under tensile stress. Generally, testing is carried out such that the maximum tensile stress is measured, and

$$S = \frac{n}{N+1} = 1 - e^{-V\left(\frac{\sigma - \sigma_u}{\sigma_0}\right)^{m+1}}$$

where S is the failure probability of a specimen of rank n, in a total sample N. The material constants σ_0 and m may be obtained by linearizing the equation logarithmically and measuring the slope and intercept. This has been carried out using a least mean squares fit to the experimental data. The value of σ_u can be obtained by computing the maximum value of the correlation coefficient with arbitrary values of σ_u. For most brittle ceramic materials $\sigma_u = 0$.

The experimental data and best fit curve are shown in Fig. 3, the constants used to generate the best fit curve being tabulated below.

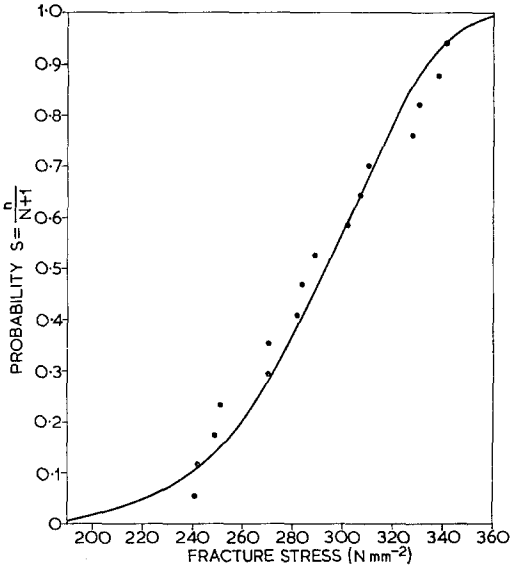

Figure 3 Strength distribution for β-alumina ceramic rings in the "as-fired" condition.

TABLE I Weibull constants and strength data for β-alumina

Mean fracture stress (N mm^{-2})	290.5
Standard deviation (N mm^{-2})	33.75
σ_0 (N mm^{-2})	305.9
m	9.2
Correlation coefficient	0.962

Figure 4 Large particle occurring on the fracture surface of a β-alumina test specimen.

6. Crack nuclei

Fracture in a ceramic material is very often nucleated at a free surface, since it is often at a surface that the maximum tensile strength arises. This is a consequence of the inability of a brittle material to absorb localized strain by micro-plastic deformation.

Surface examination of a ceramic for a crack nuclei is often unrevealing. However, on examination of a fractured surface using a plastic-carbon replica, evidence of a possible crack source can be obtained. An example is shown in Fig. 4; the large grain in the micrograph having a maximum dimension of $\sim$10 μm. Since this was a random area, there must be a flaw distribution containing both smaller and larger particles. Due to the nature of a replica it is not possible to determine whether the particle is an impurity, a large grain, or a poorly sintered region.

Substituting values of $\gamma_I = 25$ J m^{-2}, $\sigma = 300$ N mm^{-2} and $E = 1.6 \times 10^{11}$ N m^{-2}, into the Griffith formula (Equation 1), an estimate of the crack length $C \simeq 25$ μm is obtained, which is the same order of size as the large particles in the micrograph. There is no conclusive evidence that cracks start in these large particles, and it is possible that nuclei may grow by the dislocation mechanisms proposed by Gilman [10], particularly as dislocation motion can occur on the basal plane [6]. Providing a continuous defect $\sim$25 μm long could be produced then fracture would occur. With the fine material used in the present investigation an important factor would be the ability of a crack to move across the grain boundary and propagate either through the adjacent grain or along the grain boundary. Both types of crack growth have been observed.

Cracks traversing single grains were often seen in the thin foils used in transmission electron microscopy. Although not typical of cracks in bulk material they provide a useful picture of a possible nucleation and growth route. The progressive growth of a crack nuclei from a fraction of a grain length to traverse a whole grain and finally a crack many grains in length is shown in Fig. 5 a and b.

7. Material behaviour at a crack tip

As stated earlier the surface energy or fracture initiation energy γ_I of the Griffith equation is made up of a number of terms. Several geometrical factors have been observed using TEM which contribute to γ_I. Lamination of the material in the region of fracture has been observed in thin foils of β-alumina (Fig. 5a). Cracks arise due to thermomechanical stresses set up by the electron beam or by stress relief

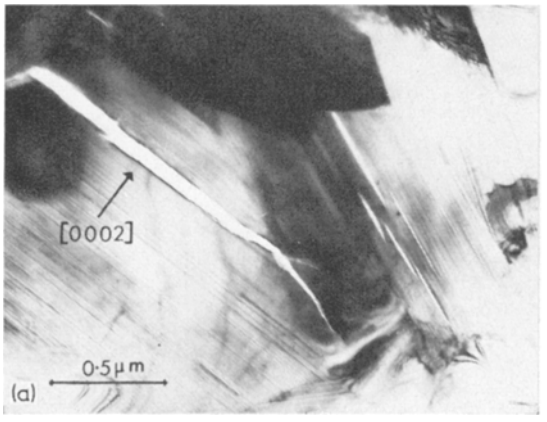

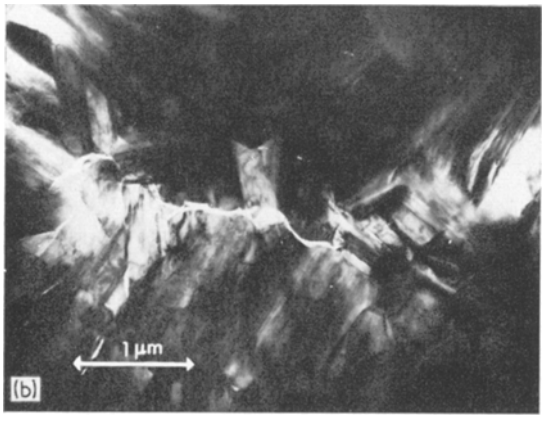

Figure 5 Stages of crack propagation in the basal plane of grains in alumina thin foils. (a) Microcracks smaller than a grain diameter causing lamination and typical microcracks across a whole grain; (b) a crack which has propagated over many grain lengths.

during the ion-beam thinning or during transfer to the electron microscope and are usually present in some parts of the thin foil specimen. In these foils the plane of the crack may be determined from a selected area diffraction pattern. Invariably the fracture path is along a basal plane. Such behaviour is not unexpected when the crystal structure of β-alumina is considered. There is only one quarter of the number of Al—O bonds across the mirror plane as compared with the number of bonds in the close packed oxygen ion layers of the spinel blocks.

On reaching a grain boundary, the crack must change direction to move along the lowest energy path. Often this is not possible, and for continued growth, the crack will have to move along higher energy cleavage planes. Examples

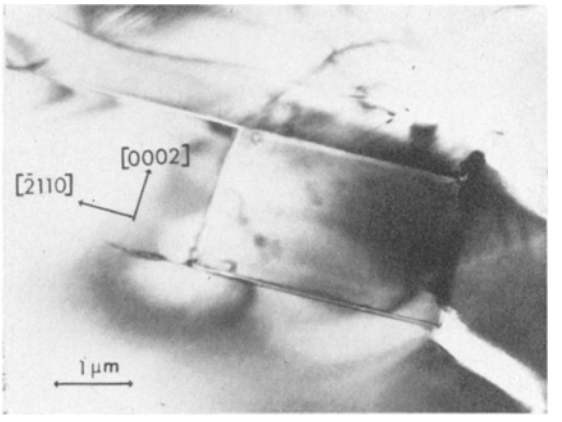

Figure 6 Change of the fracture path from the low energy basal plane to a higher energy plane, the crack starting at the bottom right hand corner of the micrograph and turning through ninety degrees before being arrested.

of the transfer from one plane to another are shown in Fig. 6. To obtain these results larger grain material was examined. In this case stresses sufficiently large were generated over areas where stress relief by fracture on basal planes was not geometrically feasible, a fracture path along alternative crystallographic planes becoming necessary.

Where the foil plane has a degree of crystallographic symmetry, such as the basal plane, visible cracks will occur on non basal planes, and changes in crack direction can occur along similar types of plane. Such behaviour is shown in Fig. 7, the crack having moved along $(1\bar{2}10)$ and changed direction to move along $(11\bar{2}0)$.

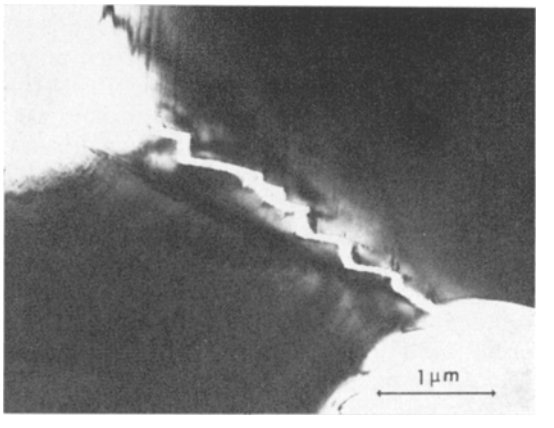

Figure 7 Microcrack in a plane inclined at a large angle to the basal plane, changing direction: the crack occurs near a grain boundary and in a narrow bridge between the thin areas in a foil.

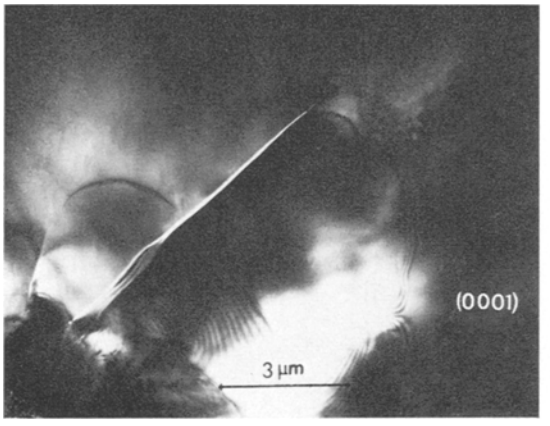

Figure 8 Transfer of a crack tip, during growth, off a crystallographic plane.

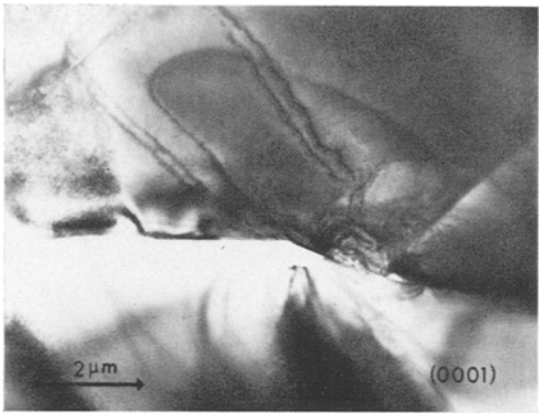

Figure 9 Dislocations in the basal plane at the tip of a crack in a monofrax single crystal. Further dislocations were visible by slight tilting of the specimen.

Another geometrical factor contributing to the increase in γ_I can be seen in Fig. 8. Here the cleavage crack tip divides and appears to move off a particular crystallographic plane, increasing both surface area and the specific surface energy.

Plastic deformation at and ahead of a crack tip is a well-known phenomena and has been observed in materials as brittle as α-alumina [18] Magnesium oxide [19] and silicon carbide [20]. Dislocation movement on the basal plane of β-alumina has recently been observed at ambient temperatures in the electron microscope [6] and significant strains observed in the single crystals examined.

Observation of basal dislocations near basal cleavage crack tips is difficult, due to the dislocation being viewed end on. However, when fracture occurs on non-basal planes such defects would be expected to be more visible. Fig. 9 shows dislocations in the basal plane at a crack tip. Two or more contrast conditions are necessary to give an overall view of the dislocation networks present, since the varying specimen thickness alters the diffraction conditions [21]. It can be seen that the dislocations are separated into two or four partials as would be expected [6].

Dislocation multiplication on tangle formation with the resulting increase in γ_p is not feasible in β-alumina due to the limited slip systems. However, the free surface energy of β-Al_2O_3 is 1.5 J m^{-2}, a value seventeen times less than the measured fracture initiation energy. The geometric factor, ϵ, is, from examination of fractographs, obviously significant, but certainly cannot account for the large difference in values. Although cross-slip and dislocation multiplication of β-alumina is not possible, due to crystallographic limitations [7], the ease of dislocation generation and movement on the basal plane in front of a crack and on basal planes adjacent to the crack plane as lamination occurs could account for the extra energy absorbed during the fracture process.

The similarity in values of the fracture initiation energy and the work of fracture suggests that the mechanisms in nucleation and propagation are probably similar. Since all the geometrical and dislocation mechanisms discussed above have been observed to take place after a crack has propagated and stopped, it should be reasonable to suggest that they could also occur around crack nuclei at fracture initiation.

8. Conclusions

1. The fracture strength of a fine grained β-alumina (< 2 μm) is 290 N mm^{-2}, and can be described by the Weibull distribution function.

2. The fracture initiation energy and work of fracture have similar values of $\sim$25 J m^{-2}.

3. Possible fracture nuclei and small cracks have been examined in thin films of β-Al_2O_3 using TEM. Most microcracks occurred on the basal plane. Crack transfer to alternative higher energy planes and off crystallographic planes was observed.

4. Dislocation generation was observed ahead of crack tips on the basal plane. Lamination of crystals by basal plane cracking was also seen to

occur, both these mechanisms forming major contributions to the fracture energies.

Acknowledgements

The helpful discussion of Dr I. W. Jones and Mr L. J. Miles is appreciated. The paper is published by permission of the Electricity Council.

References

1. C. A. BEEVERS and M. A. S. ROSS, *Z. Krist.* **95** (1936) 472.
2. J. THERY and D. BRIANCON, *Rev. Haute. Temp. Refract.* **1** (1964) 221.
3. G. YAMAGUCHI and K. SUZUKI, *Bull. Chem. Soc. Japan* **41** (1968).
4. J. T. KRUMMER, *Prog. Solid State Chem.* **7** (1972) 141.
5. I. W. JONES and L. J. MILES, *Proc. Brit. Ceram. Soc.* **19** (1971) 161.
6. Y. LE CARS, J. THERY and R. COLLONGUES, *Rev. Int. Hautes Temp Refract.* **9** (1972) 153.
7. R. STEVENS, *J. Mater. Sci.* **9** (1974) 801.
8. A. A. GRIFFITH, *Phil. Trans. Roy. Soc.* **A 221** (1920) 163.
9. E. OROWAN, "Fatigue and Fracture of Metals" (Wiley, New York, 1950).
10. J. J. GILMAN, *J. Appl. Phys.* **34** (1960) 3335.
11. M. G. TATTERSALL and G. TAPIN, *J. Mater. Sci.* **1** (1966) 296.
12. J. CONGLETON, N. J. PETCH and S. A. SHIELDS, *Phil. Mag.* **19** (1969) 160, 795.
13. B. J. HOCKEY, *J. Amer. Ceram. Soc.* **54** (1971) 223.
14. S. A. BORTZ and T. B. WADE, Analysis and Review of Mechanical Testing Procedures for Brittle Materials. Mechanical Testing Procedure for Brittle Materials IITRI March (1967).
15. S. TIMOSHENKO and J. N. GOODIER, "Theory of Elasticity" 2nd Edition (McGraw-Hill, New York, 1951).
16. F. W. SHARMAN, The Stress of Elasticity in Ceramic Rings in the Diametral Compression Test, ECRC/MM14 (1972).
17. W. WEIBULL, Ingeniorsvetenskapsakadamiens Handliger (Stockholm) No. 153 1 (1939).
18. R. J. STOKES, T. L. JOHNSON and C. H. LI, *Phil. Mag.* **3** (1958) 718.
19. M. N. SINHA, D. J. LLOYD and K. TANGRI, *J. Mater. Sci.* **8** (1973) 116.
20. R. STEVENS, *ibid* **5** (1970) 474.
21. P. B. HIRCH, A. HOWIE, R. B. NICHOLSON, D. W. PASHLEY and M. J. WHELAN, "Electron Microscopy of Thin Crystals" (Butterworth, London, 1965).

Received 16 October 1973 and accepted 7 January 1974.